Article

Not peer-reviewed version

Assessing the Post Fire Recovery of Mined Under Temperate Highland Peat Swamps on Sandstone (THPSS)

Monia Anzooman *, Phill McKenna, Natasha Ufer, Thomas Baumgartl, Neil McIntyre, Mandana Shaygan

Posted Date: 25 October 2024

doi: 10.20944/preprints202410.2016.v1

Keywords: Normalised Differenced Vegetation Index (NDVI); Soil moisture index (SMI); Sydney Basin; Upland swamps; Wildfire

Article

Assessing the Post Fire Recovery of Mined Under Temperate Highland Peat Swamps on Sandstone (THPSS)

Monia Anzooman [1,*], Phillip McKenna [2], Natasha Ufer [3], Thomas Baumgartl [4], Neil McIntyre [1] and Mandana Shaygan [1]

[1] Centre for Water in the Minerals Industry, Sustainable Minerals Institute, The University of Queensland, Brisbane, Qld 4072 Australia; n.mcintyre@uq.edu.au (N.M.); m.shaygan@uq.edu.au (M.S.)
[2] Centre for Mined Land Rehabilitation, Sustainable Minerals Institute, The University of Queensland, Brisbane, Qld 4072 Australia; p.mckenna@cmlr.uq.edu.au
[3] Department of Environment, Science and Innovation, Queensland Government, Brisbane, Qld 4001 Australia; natasha.ufer@des.qld.gov.au
[4] Future Regions Research Centre, Federation University, Gippsland, VIC 3841 Australia; t.baumgartl@federation.edu.au
* Correspondence: m.anzooman@uq.edu.au

Abstract: The Temperate Highland Peat Swamps on Sandstone (TPHSS), unique to the Sydney Basin of Australia, were burnt during the 2019-2020 wildfire season. This study assessed the post fire recovery of swamps and the ability of remote sensing technique to determine the post-fire recovery patterns. Specifically, the study investigated differences in fire recovery between swamps where groundwater level and soil moisture content have been impacted by underground mining and unimpacted by mining. Two mined and one non-mined under swamps were investigated. Soil moisture measurements were taken at five sites and previously conducted vegetation field surveys (from 2016 to 2022) were used. Using remote sensing information, Normalised Differenced Vegetation Index (NDVI) and Soil Moisture Index (SMI) time-series were calculated and compared with ground data to map responses over the swamps following the fire impact. This study revealed that hydrological conditions of swamps have a direct effect on post-fire recovery of swamps, with slower recovery in mined under swamps compared with non-mined under swamps. This study indicated that NDVI and SMI indices can exhibit the recovery pattern of swamps in terms of vegetation and hydrology. However, the evaluation of recovery pattern of a specific vegetation species requires a frequent field survey.

Keywords: Normalised Differenced Vegetation Index (NDVI); Soil moisture index (SMI); Sydney Basin; Upland swamps; Wildfire

1. Introduction

The Temperate Highland Peat Swamps on Sandstone (THPSS) are unique ecosystems within the Sydney Basin Bioregion of Australia that are characterized by the development of peat overlying Triassic Sandstone formations at elevations ranging between 600 and 1200m above sea level [1]. These swamps are a distinctive feature of the region, habitat to unique vegetation that thrives on high groundwater levels, high soil moisture content, and organic-rich sediments [2,3]. Some of the THPSS are situated over underground mining areas, and subsidence due to the mining and associated fracturing of the sandstone can be a reason for changes in the THPSS hydrology [4–6]. A concern often raised is that mining-induced drainage of THPSS reduces their resilience to wildfires [1].

Wildfires are not uncommon in areas containing THPSS. The swamps typically exhibit high resilience to fire, primarily due to their elevated soil moisture levels and the capacity to support swift vegetation regrowth [1,7]. However, there is a lack of understanding on the resilience of THPSS affected by underground mining and subsequently subjected to wildfires. Some studies [1,8,9] have suggested that drier soil moisture conditions may reduce swamp resilience to fire, leading to an increased risk of permanent damage and the loss of vegetation and ecological function. However, there is little evidence to support this. Therefore, understanding the post-fire recovery of mined

 doi:10.20944/preprints202410.2016.v1

under swamps and non-mined under swamps is critical. It has been hypothesised that post fire recovery of mined-under swamps is different from the post fire recovery of non-mined-under swamps.

Remote sensing provides an innovative methodology for quantifying fire severity and vegetation changes both temporally and spatially [10]. Historically, fire severity mapping utilized moderate to coarse spatial resolution Landsat imagery (i.e. 30 m pixel) [11–13]. Satellite imagery can now reach pixel resolutions of three meters [14]. Therefore, the utilization of remote sensing to characterize fire impacts is gaining prevalence [15]. Beyond traditional fire severity mapping with multispectral imagery, satellite thermal bands offer the capacity to generate spatially comprehensive measurements of surface environmental conditions, including land surface temperature (LST) and soil moisture index (SMI). This may offer opportunity to improve understanding of post fire recovery of THPSS swamps. Studies have used thermal imagery to evaluate wildfire events in landscape scale [16–19]. However, there remains a significant knowledge gap concerning the value of multispectral and thermal imagery for this purpose, particularly at the plot scale (<500m^2) and the local scale (1km^2).

This study addresses the above research gaps by investigating fire severity and post fire soil moisture and vegetation changes of three THPSS swamps. This study aims (i) to determine the post fire recovery patterns of mined under and non-mined under THPSS swamps, and (ii) to explore the potential of remote sensing data to assess post fire recovery of THPSS swamps.

2. Materials and Methods

2.1. Site Description

The three swamps, which were selected for this study, included two swamps in the Newnes Plateau (Swamps A and B) and one swamp in Upper Nepean (Swamp C) regions of the Sydney Basin Bioregion (Figure 1). These swamps have been chosen due to their accessibility, underground mining activities, and historical fire events. Swamps A and B (with monitoring locations A1, B1 and B2) were mined under (Figure 1a). Conversely, swamp C (with one monitoring location: C1) was not mined under (Figure 1b). A large wildfire which was unprecedented in scale and severity moved through Newnes Plateau in December 2019 and burnt Swamps A and B as well as other swamps. A wildfire also burnt Swamp C in May 2020. The combination of mining history and the occurrence of these extensive wildfires provides a unique context for studying the post-fire recovery dynamics of the selected swamps, offering valuable insights into the interplay of mining and wildfire on this ecosystem.

The study swamps have warm summers and cool winters [2]. The long-term average annual rainfall was 793 mm and 1124 mm for the Newnes Plateau and Upper Nepean areas, respectively [20]. The average annual minimum and maximum temperatures at Newnes Plateau and Upper Nepean were -1.1 °C and 23.5 °C and 1.7 °C and 29.3 °C [20]. Daily rainfall and air temperature data of the study locations before and after the fire events are presented in Figure A1.

 doi:10.20944/preprints202410.2016.v1

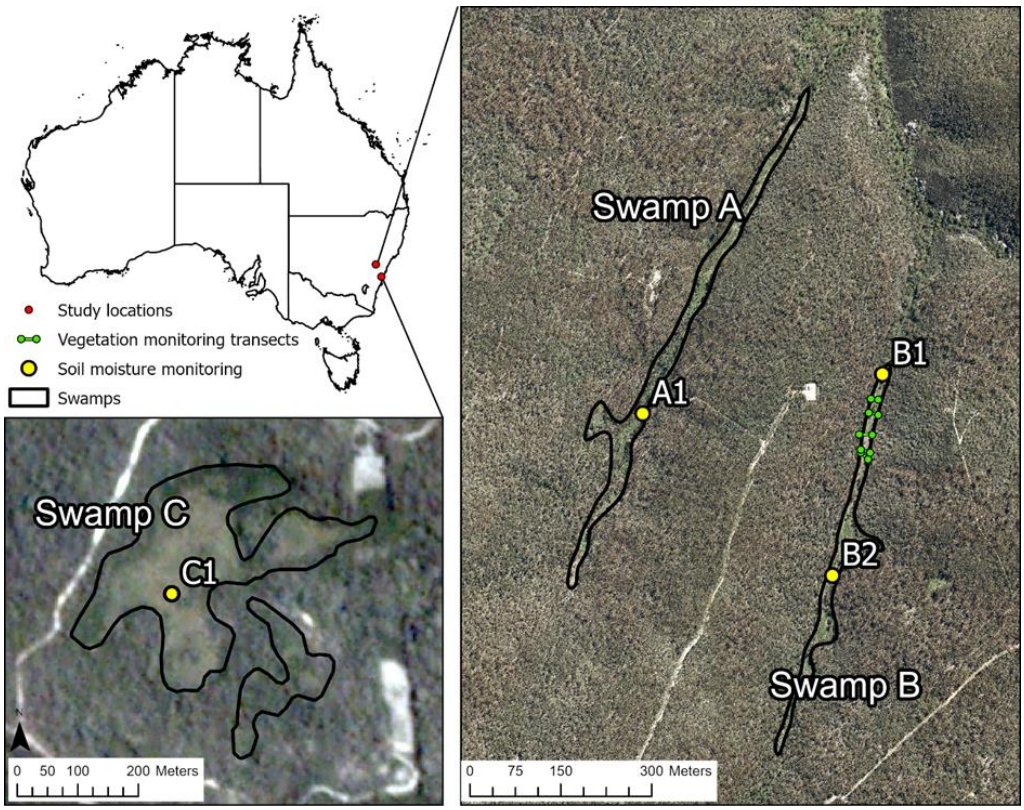

Figure 1. Aerial photo indicating the study locations in (a) Newnes Plateau (mined-under swamps): Swamp A (8.9 ha) and Swamp B (5.09 ha), (b) Upper Nepean (non-mined-under swamp): Swamp C (9.02 ha). The green points on Swamp B represent the vegetation monitoring transects. A1, B1, B2 and C1 represent the soil moisture monitoring points.

2.2. In Situ Soil Moisture Monitoring

The topsoil moisture fluctuations at sites A1, B1 and B2 were measured using soil water potential meters (tensiomark [21]) installed at 10 cm below the surface. For site C1, the topsoil moisture fluctuations were measured using a Sentek soil moisture sensor also at 10 cm below the surface. The water potential data were converted to volumetric water content values using soil water retention curve parameters from the same swamps mentioned in Shaygan, Baumgartl and McIntyre [2]. The Sentek sensor provided volumetric water content based on the calibration curves in Sentek Pty Ltd [22].

2.3. Vegetation Monitoring

Field vegetation surveys were conducted yearly for Swamp B from 2016 to 2022 using the five transects (10 survey points) indicated in Figure 1. Surveys for swamps A and C could not be conducted due to access restrictions as a result of COVID-19. However, the vegetation communities within the study swamps were similar as mentioned in Young [1]. Thus, the validation from Swamp B is deemed to be applicable to all the study swamps (Swamp A, B and C).

2.4. Remote Sensing Metrics

Spectral indices for remote sensing, such as NDVI (the Normalized Difference Vegetation Index), and SMI (the Soil Moisture Index), were computed to investigate key indicators of vegetation damage, vegetation cover and soil moisture changes.

The NDVI value, which has been widely employed for assessing vegetation cover, health, and vigor [23–25], correlates with greenness and biomass, and utilizes RED and NIR (the Red and Near-Infrared) bands of the electromagnetic spectrum (Equation 1).

 doi:10.20944/preprints202410.2016.v1

$$\mathrm{NDVI} = \frac{\mathrm{NIR} - \mathrm{RED}}{\mathrm{NIR} + \mathrm{RED}} \quad (1)$$

Fire severity maps were generated using high spatial resolution surface reflectance Planet imagery (3 m) [14], with the Swamp A and B pre-fire and post-fire images acquired on December 3, 2019 and February 27, 2020, respectively, and the Swamp C pre-fire and post-fire images acquired on May 8 and 10, 2020, respectively (Table A1). Differenced NDVI rasters were computed through image differencing in ArcGIS Pro, utilizing pre- and post-fire images of the sites to create fire severity rasters, as per Equation 2:

$$dNDVI = prefireNDVI - postfireNDVI \quad (2)$$

The resulting rasters were subsequently classified into five categories: unburnt, low, moderate, high, and extreme severity (Table A2). Using preliminary dNDVI fire severity maps, 50 points were randomly assigned to each class and ranked according to the fire severity class descriptions, as outlined by Gibson, et al. [26] (Table A2), and through API (aerial photo interpretation) of high-resolution aerial imagery captured both before the fire and after the fire. Class thresholds were re-evaluated based on API, and an error matrix was generated to calculate the accuracy of the fire severity maps. The error matrix was not able to be produced for Swamp C. However, as the vegetation communities are similar in the study swamps [1], the error matrix from Swamp A and B is applicable to Swamp C.

The SMI is defined as the proportion of the difference between the current soil moisture and the permanent wilting point to the field capacity and the residual soil moisture [27]. The index values range from 0 to 1 with 0 indicating very dry conditions and 1 indicating soil moisture at field capacity [27]. The SMI value of each study site is the value of single pixel representing the relevant site. The soil moisture index is primarily derived from the land surface temperature (LST) and vegetation indices (NDVI) of the region under study. The SMI was calculated on empirical parameterization of the relationship between LST and NDVI using Equation 3.

$$SMI = \frac{LST_{max} - LST}{LST_{max} - LST_{min}} \quad (3)$$

Where LSTmax and LSTmin are the maximum and minimum surface temperatures for a given NDVI and LST is land surface temperature derived from Landsat 8 bands 10 and 11.

Land Surface Temperature (LST) is defined as radiative skin temperature of any land derived from solar radiation [28]. Landsat 8 OLI (Operational Land Imager) satellite imagery was used to calculate the LST and Bands 10 and 11 were used to capture reflectance in the thermal infrared (10.6-11.19 μm and 11.5-12.51 μm respectively). The Landsat series of satellites derived from GEE (Google Earth Engine) provided LST estimates at a resolution of 30 m using algorithm following Ermida, et al. [29] and was suitable for local/ regional scale study sites. The LST retrieval algorithm used here requires prescribed values of surface emissivity [30]. Surface emissivity over time can vary due to annual and inter-annual variations in vegetation density. Therefore, a vegetation adjustment was applied using NDVI and fraction of vegetation cover was derived to calculate LST [31]. The methodology for deriving LST was described in Ermida, et al. [29].

The workflow diagram indicating the steps of calculating NDVI, dNDVI and SMI is shown in Figure A2. Time series of NDVI and LST were extracted from Google Earth Engine (GEE) using Landsat 8 surface reflectance values.

2.5. Validation of Remote Sensing Indices

The SMI values were extracted from the corresponding pixels measured soil moisture values collected in situ to derive the correlation between measured volumetric soil moisture contents and SMI values. This provides validation and indicates the accuracy of the calculated SMI values by reflecting how well the SMI index represents soil moisture content.

Validation of NDVI data was performed through the surveyed vegetation data for Swamp B. The GPS coordinates of the vegetation monitoring locations were used and, their NDVI data (relevant pixel) were extracted. A correlation was established between the total plant cover and NDVI data of

 doi:10.20944/preprints202410.2016.v1

the monitoring points to validate the NDVI data and maps. This correlation reflects how well the NDVI values represents the vegetation cover in the swamps.

2.6. Analysis

NDVI and SMI values were extracted from individual pixels corresponding with monitoring locations within each swamp and plotted against time to understand the vegetation and moisture changes pre and post fire events. Pixels were chosen from homogeneous areas where the swamp width exceeded 30 m to minimize interference from non-swamp vegetation along the swamp edges. A cloud filter of less than 5% was applied in GEE to reduce cloud interference in the plots.

3. Results

In this paper, we firstly present the dNDVI maps of the study swamps to understand the impact of fires within each swamp. Then, we present the NDVI and SMI maps followed by the NDVI and SMI time series of selected sites. This provides an opportunity to compare the vegetation cover and soil moisture changes between mined under and non-mined under swamps. This also provides an opportunity to assess the effect of fire severity on vegetation cover and soil moisture fluctuations. Finally, the assessment of remote sensing accuracy against ground data is reported.

3.1. Fire Severity of the Swamps

The imagery revealed the impact of wildfires on the swamps (Figure 2). At Newnes Plateau, Swamp B and the vegetation communities to the north experienced more severe impacts than Swamp A (Figure 2c). Meanwhile, at Upper Nepean, the central part of Swamp C was notably affected by the wildfire and burnt severely during the fire event in comparison to the surrounding areas (Figure 2f). Based on the fire severity maps, site A1 was classified as low burn severity, B1 as high burn severity, B2 as moderate burn severity and C1 as extreme burn severity (Figures 2c and f).

The error matrix for the fire severity indicated an overall map accuracy of 77% (Table A3). Within this, the high and extreme severity classes exhibited 77% and 100% user accuracy, while producer accuracy was 88% for high severity and 65% for extreme severity (Table A3). The kappa index recorded 71% (Table A3), suggesting a good agreement between the reference samples and the final severity model.

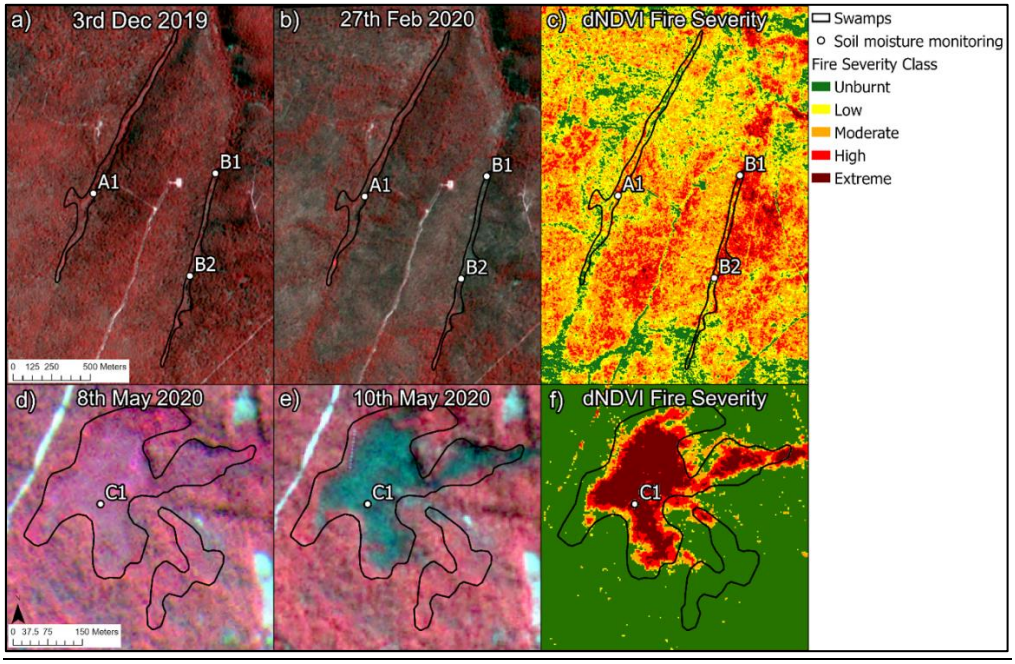

Figure 2. Planet satellite imagery showing a) CIR pre-fire, b) CIR post-fire and c) classified fire severity map using dNDVI on the Swamp A and Swamp B from Newnes Plateau and d) CIR pre-fire, e) CIR post-fire and f) classified fire severity map using dNDVI on the Swamp C from Upper Nepean. Fire

 doi:10.20944/preprints202410.2016.v1

severity maps were classified to unburnt (green colour), low burn (yellow colour), moderate burn (orange colour), high burn (red colour) and extreme burn (maroon colour).

3.2. *Vegetation Cover Changes*

A higher NDVI value represents a higher greenness and biomass of vegetation, while a lower value represents a lower greenness and biomass [23,32,33]. Swamp A vegetation communities were not severely affected by the 2019 wildfire, and the communities commenced to recover in March 2020 (Figure 3). Although swamp B and its vegetation communities to the north were affected severely, the communities to the north of swamp B commenced to recover in March 2021, in which the greenness/biomass returned approximately to the pre-fire condition in May 2022, 884 days after the fire (Figure 3). The NDVI time series of the sites in swamps A and B indicated that the changes in vegetation cover of swamps were similar before the wildfire (Figure 4). Both swamps reached a peak NDVI of 0.8 in July 2019. Then, in both, a significant reduction in NDVI values was observed from September 2019 possibly due to the drought condition (Figure 4). The NDVI values of the A1, B1 and B2 sites approached 0.38, 0.34 and 0.31 in December 2019 following the wildfire (Figure 4) and returned to pre-fire values (>0.66) in July 2022 (Figure 4). The NDVI time series for C1 in the non-mined-under swamp indicates a drop in NDVI to 0.46 after the wildfire (Figure 4). For this site, the vegetation returned to pre-fire condition after one year when the NDVI value increased to 0.81 (Figure 4 and Figure 5).

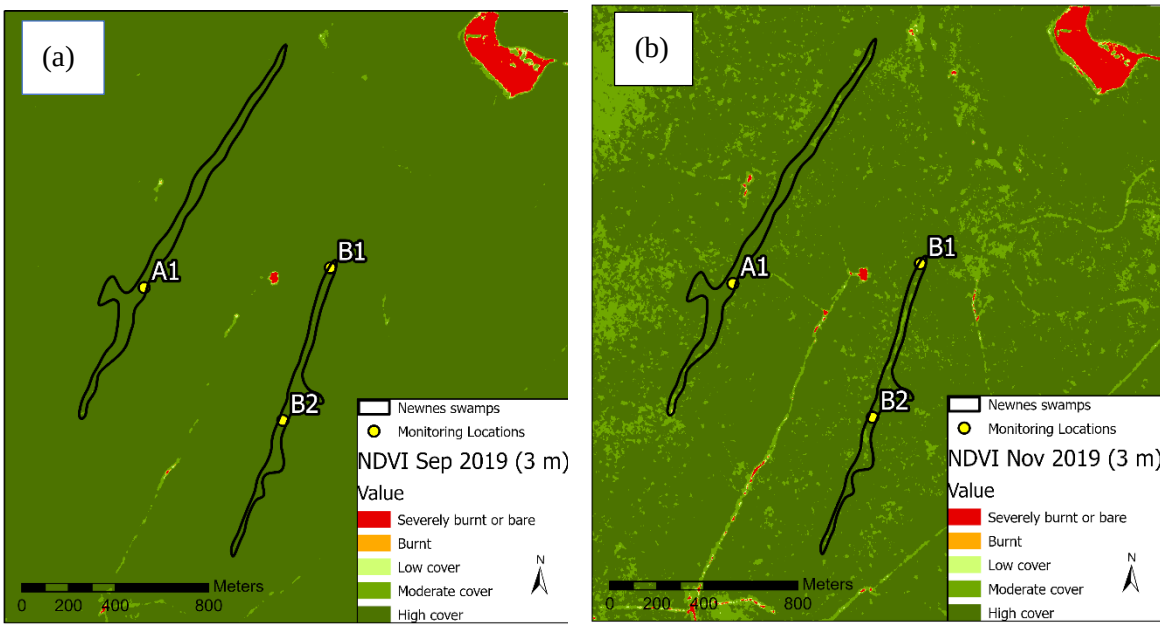

 doi:10.20944/preprints202410.2016.v1

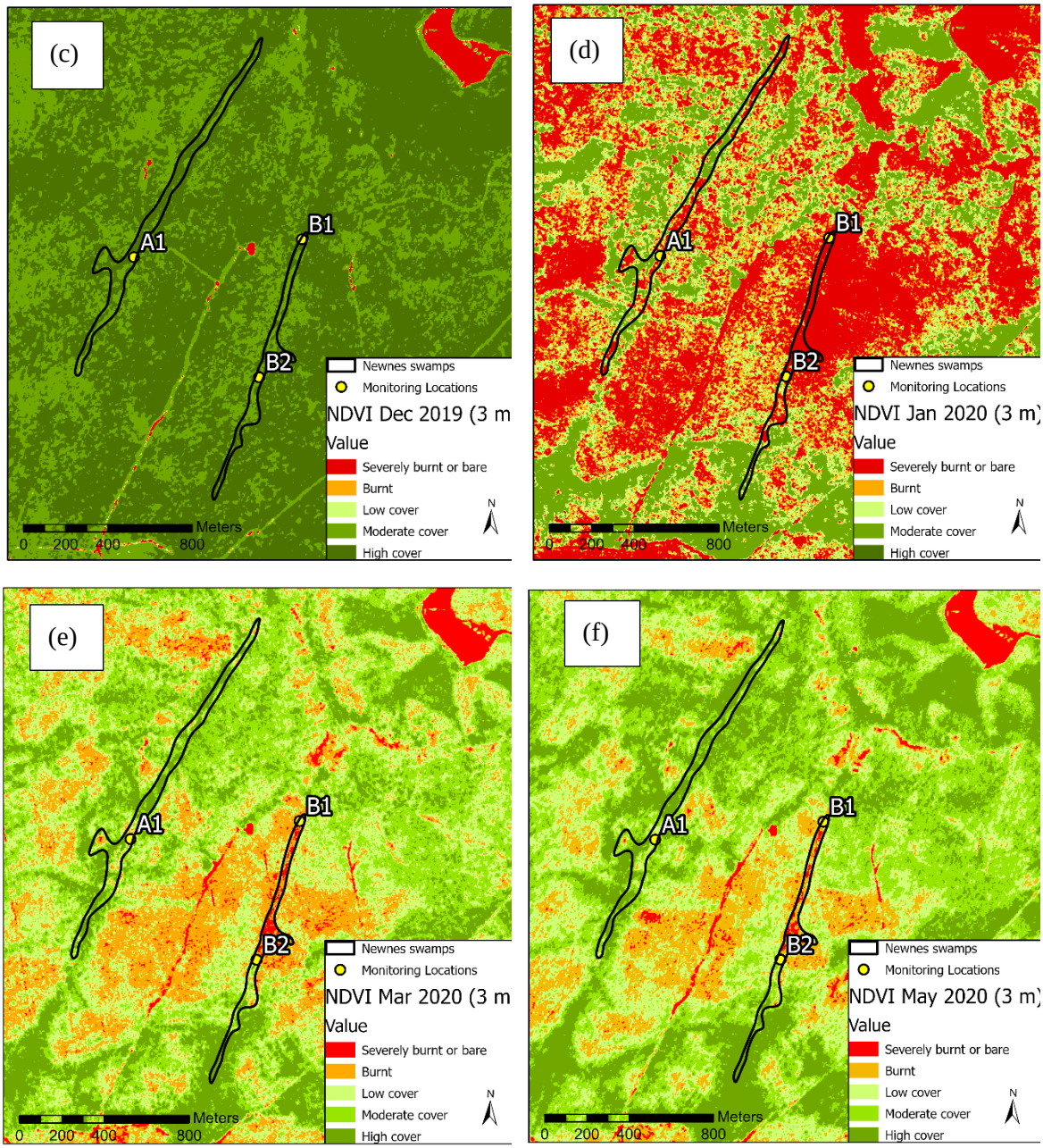

 doi:10.20944/preprints202410.2016.v1

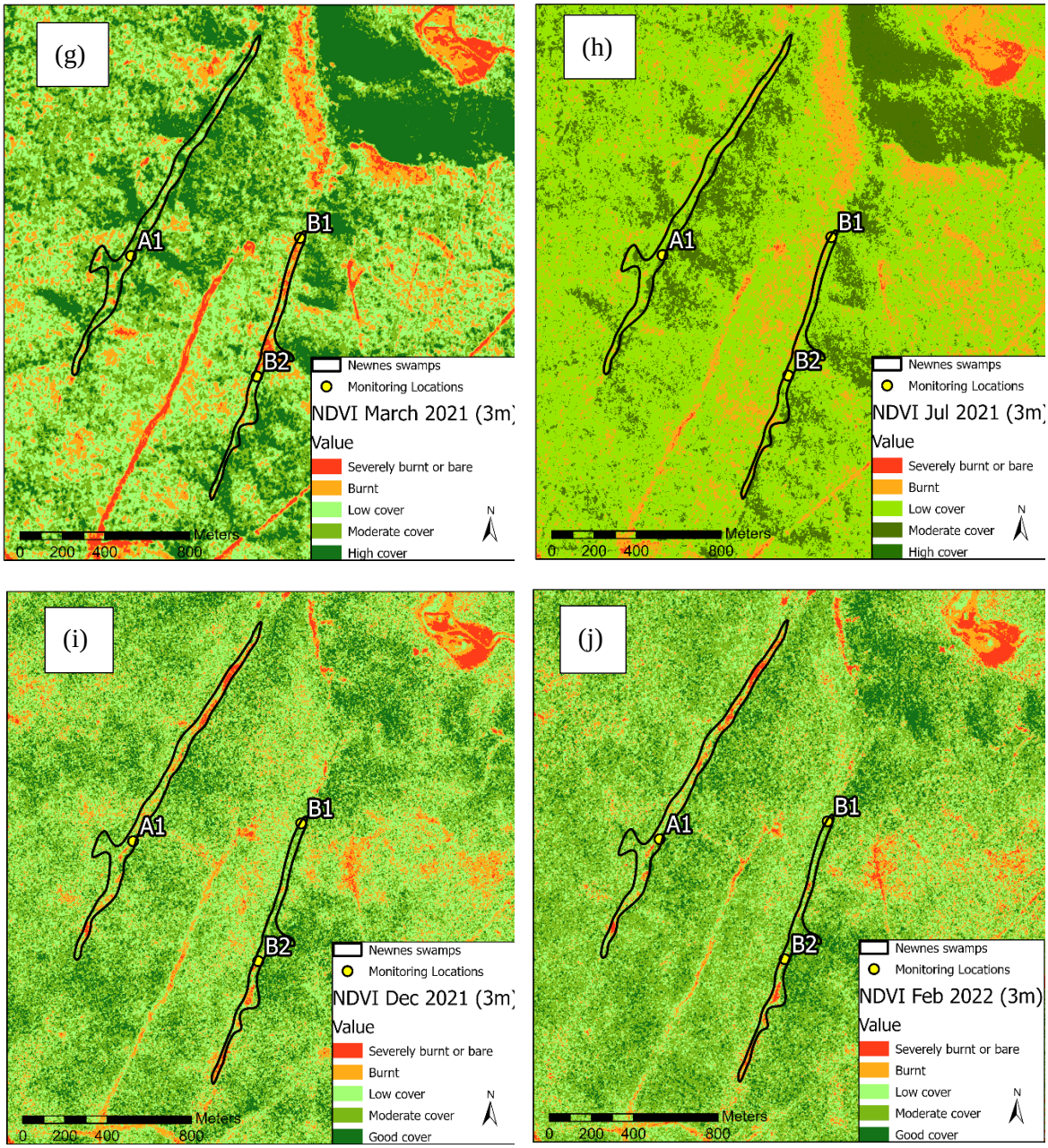

 doi:10.20944/preprints202410.2016.v1

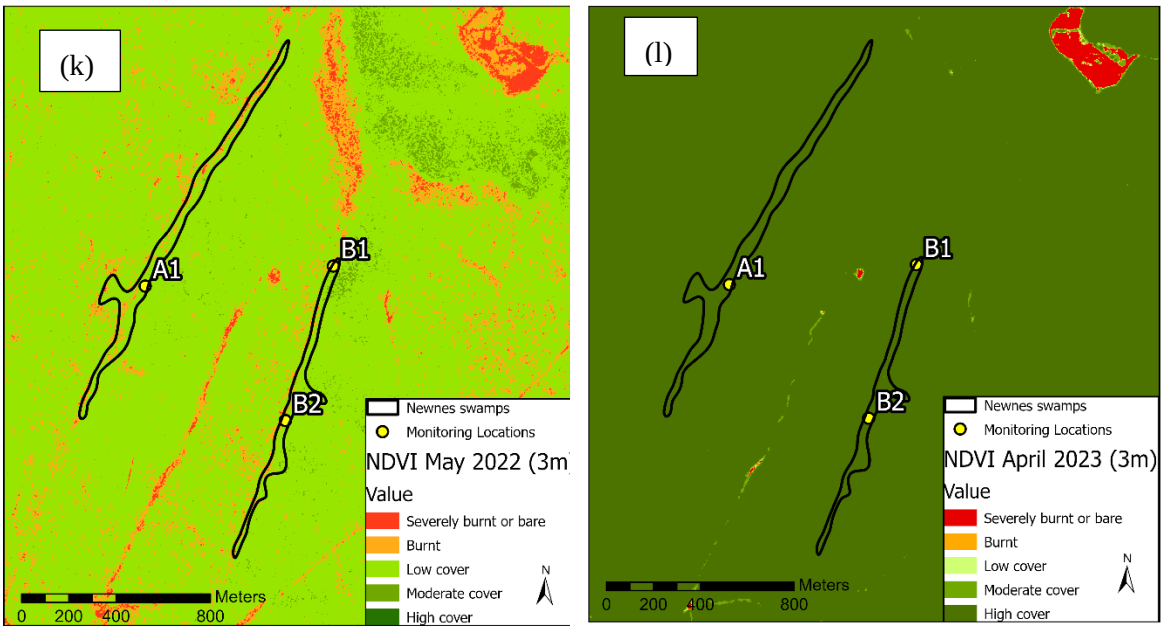

Figure 3. Planet NDVI maps for Swamps A and B from September 2019 to April 2023 (Wildfire occurred in December 2019).

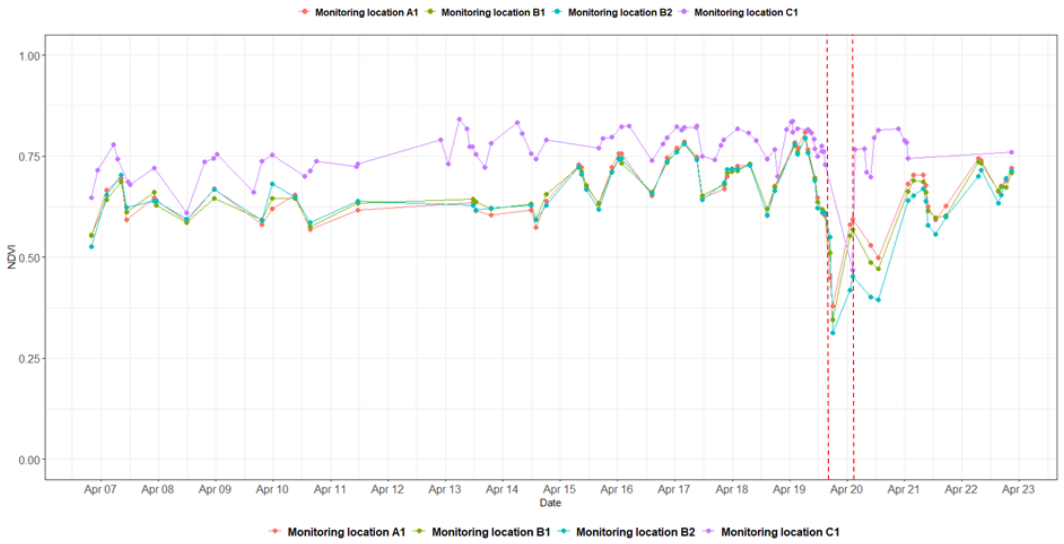

Figure 4. The NDVI time series from January 2007 to January 2023 for monitoring locations A1, B1, B2, C1. The dotted red lines represent the December 2019 fire event affected sites A1, B1, B2 and May 2020 fire event affected site C1.

 doi:10.20944/preprints202410.2016.v1

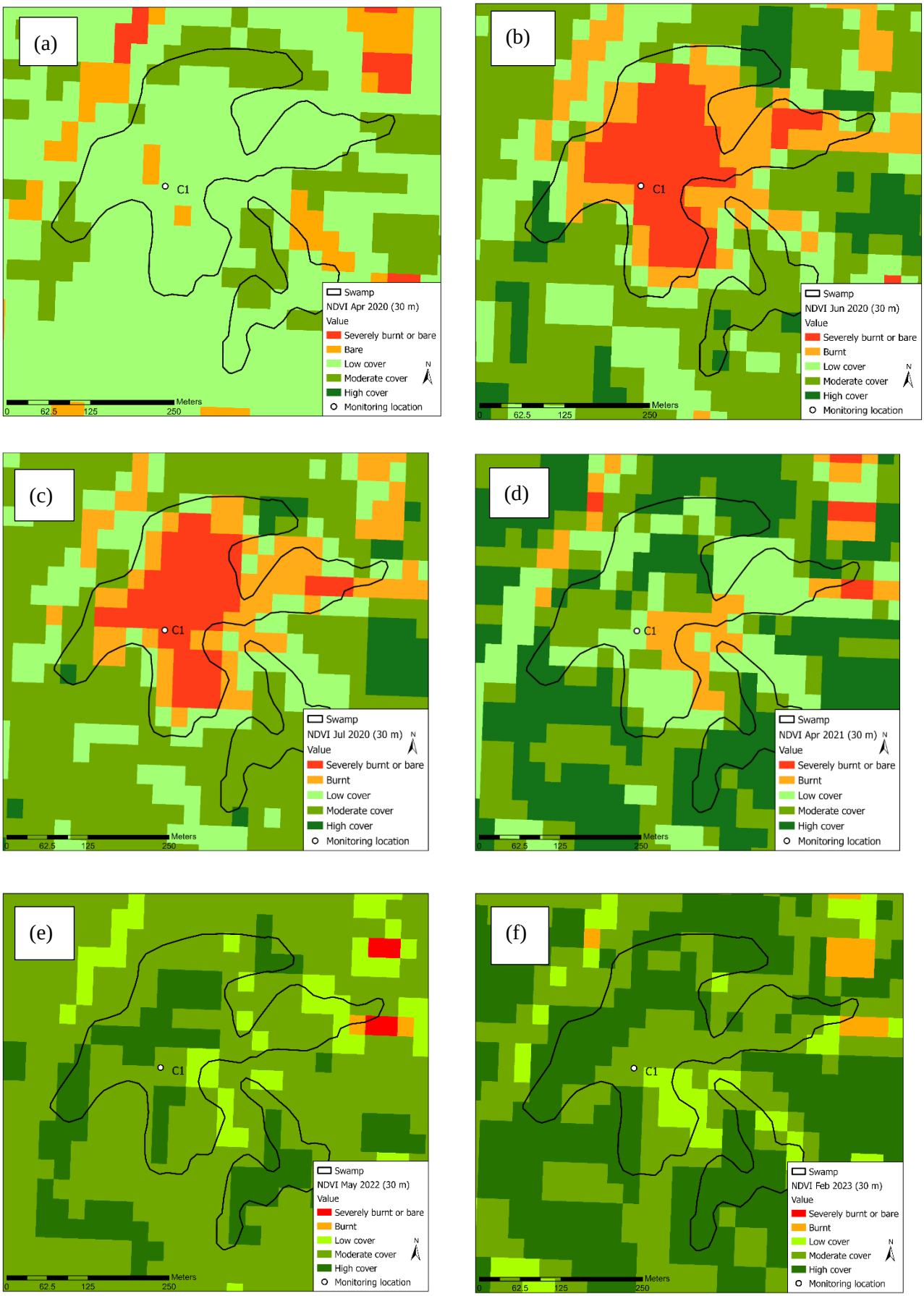

 doi:10.20944/preprints202410.2016.v1

Figure 5. Landsat NDVI maps for Swamp C from April 2020 to February 2023 (Wildfire occurred in May 2020).

3.3. Soil Moisture Index Fluctuations

Soil moisture in swamps A and B was notably lower in December 2019 (when wildfire occurred) compared to previous and following months, with SMI values as low as 0.1 in some areas (Figure 6). The SMI value for site A1 (low severity burnt site) dropped to 0.2 at the time of the fire event in December 2019 then returned to its pre-fire condition in November 2020 with a SMI value of 0.60 (Figure 6b). The SMI value then fluctuated before remaining constant between 0.6 and 0.55 (Figure 6b). For site B1 (high severity burnt site), the SMI dropped to 0.43 at the time of the fire in December 2019. Then, it increased to 0.67 in March 2020 before fluctuating a lot (Figure 6b). For site B2 (moderate severity burnt site), the SMI dropped to 0.32 during the fire before returning to pre-fire conditions with small fluctuations in March 2020 with SMI value of 0.61 (Figure 6b). The SMI value then remained stable until March 2023 for this site (Figure 6b). For site C1, the SMI value was 0.4 in August 2019, and it dropped to 0.002 as the swamp was burnt in May 2020 (Figure 7). The SMI returned to pre-fire condition in April 2021, almost a year after the bushfire, with SMI value of 0.34 and then it remained in steady condition (Figure 7).

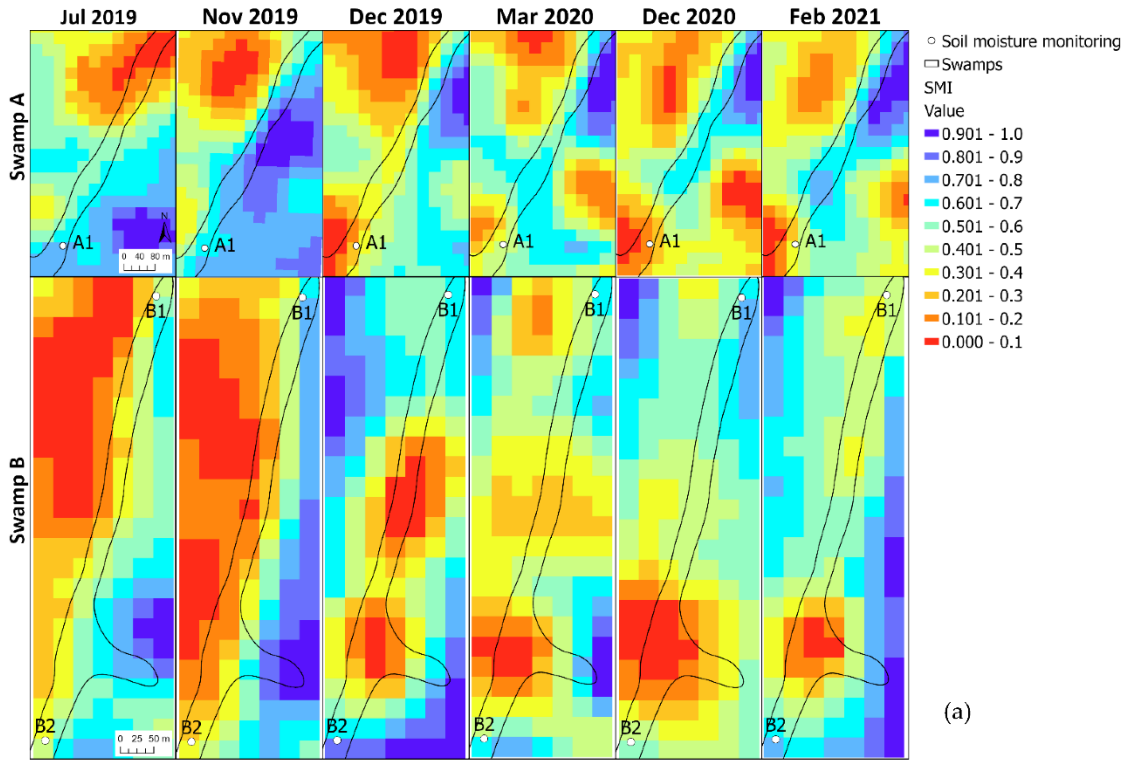

(a)

Preprints.org (www.preprints.org) | NOT PEER-REVIEWED | Posted: 25 October 2024 doi:10.20944/preprints202410.2016.v1

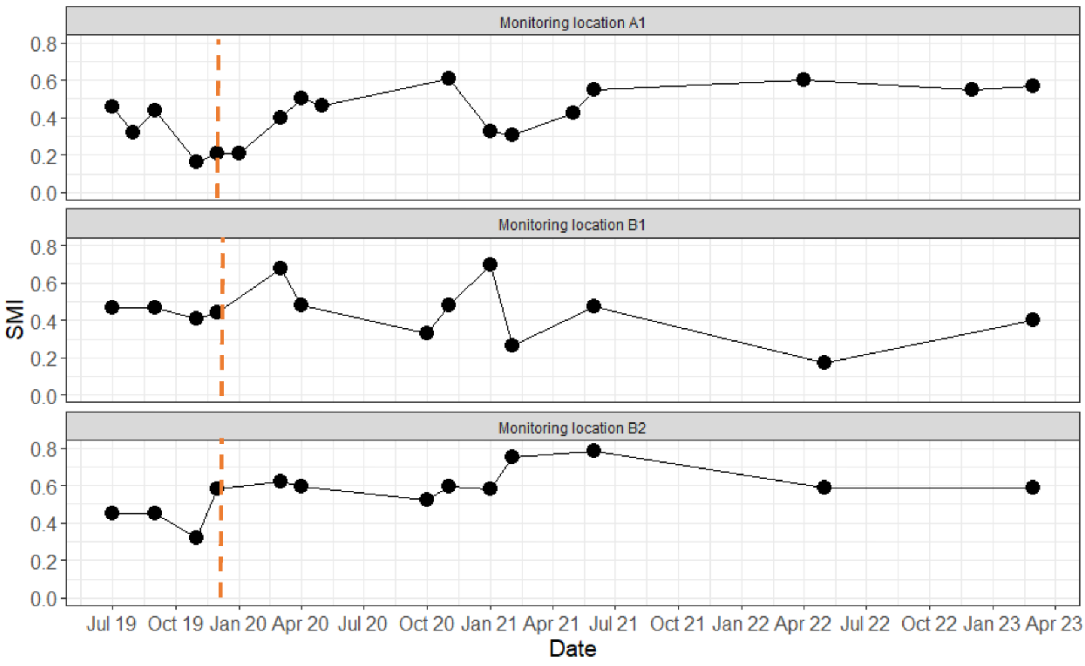

(b)

Figure 6. Soil Moisture Index (SMI) fluctuations in Newnes Plateau study swamps (a) SMI maps of Swamp A and Swamp B topsoil from July 2019 to February 2021 and (b) SMI time series for topsoil of studied sites in Newnes Plateau (monitoring locations A1, B1, B2) (the wildfire occurred in December 2019).

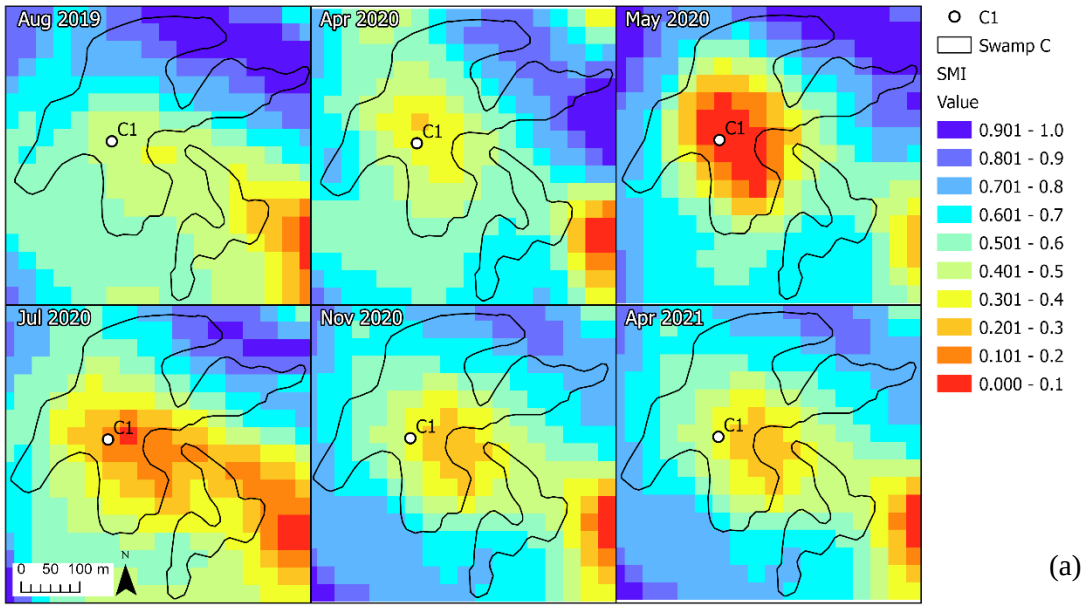

(a)

 doi:10.20944/preprints202410.2016.v1

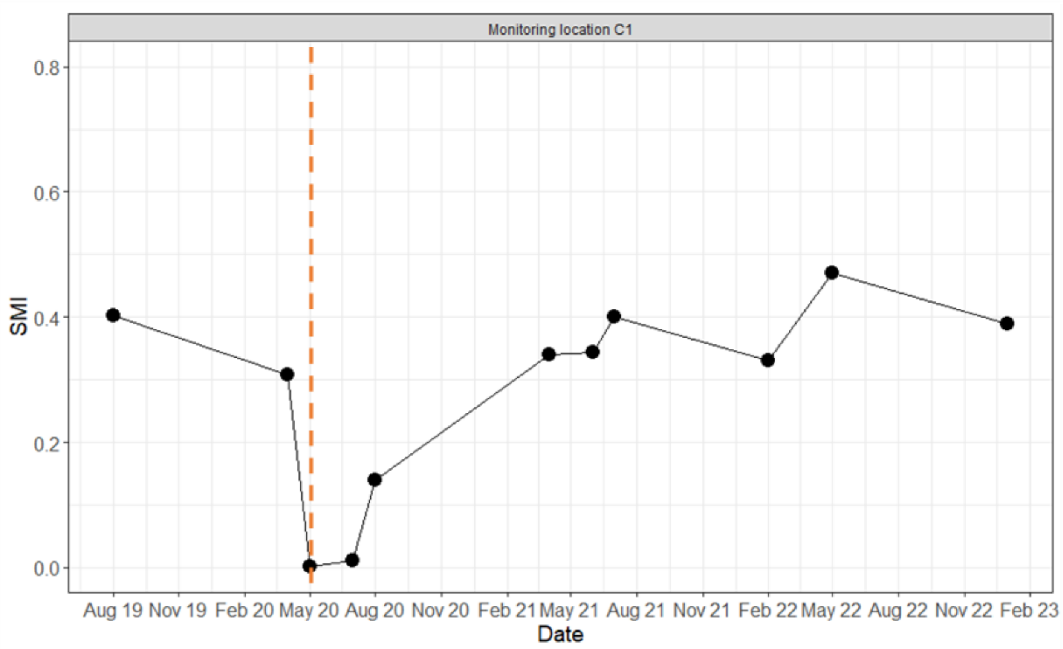

(b)

Figure 7. Soil moisture index (SMI) fluctuations in Upper Nepean study swamp (a) SMI maps of Swamp C topsoil from August 2019 to April 2021 and (b) SMI time series for topsoil of studied site in Upper Nepean (monitoring location C1). The dotted red line represents the fire event for the location (the wildfire occurred in May 2020).

3.4. Validation of Remote Sensing Metrics

Figure 8 shows the comparison of NDVI values with field-surveyed vegetation cover data from the five monitoring transects which was indicated in Figure 1. The correlation co-efficient (R2) was 0.86 indicating that the NDVI data time series and NDVI maps reasonably represent variations in vegetation cover.

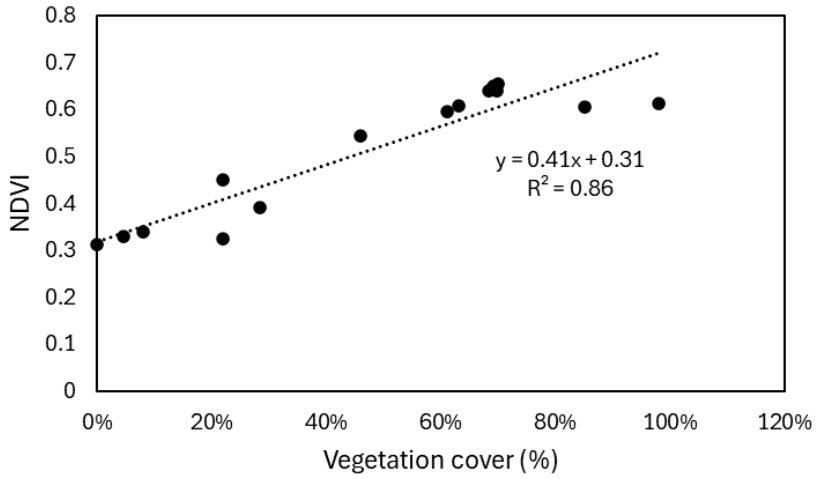

Figure 8. Correlation between observed field vegetation cover and NDVI values.

Strong correlation was observed between the measured soil volumetric moisture contents in 10 cm soil depth and SMI values, in which the correlation coefficient values were 0.7, 0.75, 0.8 and 0.97 for sites A1, B1, B2 and C1 (Figure 9).

 doi:10.20944/preprints202410.2016.v1

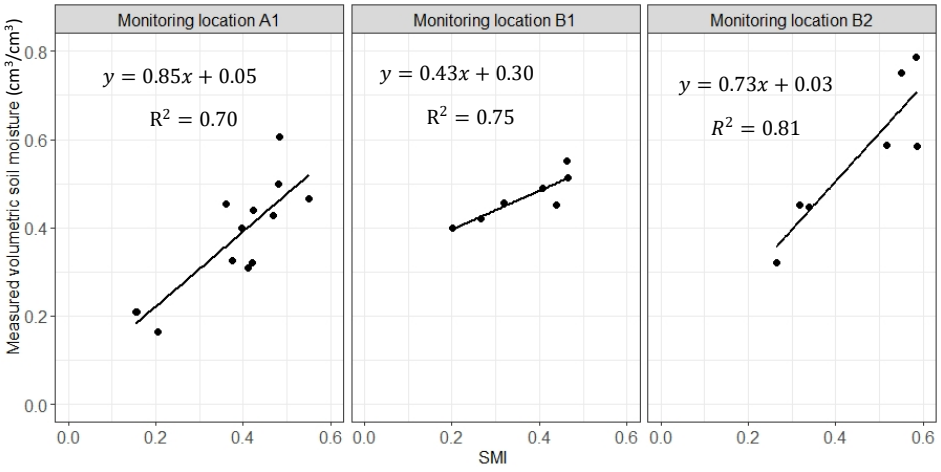

Figure 9. Correlation between the calculated Soil Moisture Index (SMI) values and measured volumetric moisture contents of the topsoil of the studied sites.

4. Discussion

4.1. Post Fire Recovery of Mined Under and Non-Mined Under THPSS

Temperate Highland Peat Swamps on Sandstone are characterized by the plant species that exhibit rapid regrowth following fires, primarily due to the high soil moisture content of these swamps [1,34,35]. However, the post fire recovery of mined under swamps and non-mined under swamps may differ. In this study, the vegetation recovery was defined as the point in time when the variation in NDVI reaches pre-fire levels. Therefore, the NDVI time series revealed that vegetation cover recovery of mined under swamps were slower compared to non-mined under swamps. The vegetation cover recovery of the swamp, which have not been mined under (i.e. Swamp C), achieved almost after one year from the fire, while a slower post-fire vegetation recovery (2.5 years) was observed for mined under swamps (i.e. Swamp A and B) (Figure 3-5). Swamp hydrology affected by underground mining appears to have the potential to influence the post fire recovery of swamps and burned sites. In this context, soil moisture, which is directly related to the rainfall, groundwater level, evaporation and evapo-transpiration, can be an indicator of swamp hydrology when similar soil types are compared [2]. Therefore, understanding soil moisture recovery of swamps can assist with comprehending the process of post fire recovery of mined under and non-mined swamps. This study indicated that the vegetation recovery of study swamps was related to their soil moisture fluctuations. The soil moisture contents of non-mined under swamp returned to the pre-fire conditions almost a year after the fire, and the mined under swamps had greater soil moisture fluctuations compared to the non-mined under swamp (Figure 6 and Figure 7). This affected post fire vegetation recovery timeline in which a quicker post fire recovery was observed for non-mined under swamps. This was in agreement with other studies [35–37], which concluded that the enhanced drainage of a peatland resulted in a drier condition and more fluctuations in soil moisture condition influencing post fire conditions of the peatlands. This study implies that the post fire vegetation recovery of swamps depends on post fire hydrology of swamps, and a higher soil moisture content can result in more rapid vegetation recovery for swamps while low soil moisture content may delay the recovery process.

The fire severity may affect the post fire vegetation recovery pattern [38–40]. Interestingly, no observable differences presented in the vegetation cover recovery of sites with different fire severities in mined under swamps (A1: low burnt; B1: high burnt and B2: moderate burnt), and the NDVI time series of these sites followed a same pattern and obtained recovery in July 2022 (Figure 4). This was possibly related to comparable soil hydrological properties among the study sites (Table A4) which induced similar hydrological changes among the sites with different fire severities. This is in contrast with Moody, et al. [41] who reported that soil hydraulic properties of high burnt areas differ significantly from those of low burnt sites, in which a greater hydraulic conductivity and porosity can be found in sites with greater fire severity.

 doi:10.20944/preprints202410.2016.v1

4.2. Remote Sensing as a Tool to Assesss the Post Fire Recovery of THPSS

Remote sensing technique can indicate vegetation cover and biomass changes both temporally and spatially using Normalized Difference Vegetation Index (NDVI) [23,32,33,42]. Therefore, this index may demonstrate and help with understanding the post fire recovery of swamps. A good correlation between monitored vegetation cover and the remote sensed value such as NDVI can validate the suitability of remote sensing technique for assessing vegetation changes over time [39,43,44]. In this study, the strong agreement between monitored vegetation cover and NDVI values (Figure 8) indicated that the NDVI values can be used to gain ecological information on THPSS swamps where a high spatial resolution is needed to accurately detect recovery in the vegetation communities after fires. Although the NDVI values cannot differentiate the recovery of each individual plant species, they can unravel broad patterns for post fire recovery of THPSS swamp communities. Understanding the recovery pattern of each individual plant species requires an intensive vegetation monitoring program (e.g. quarterly vegetation survey) including drone and field surveys. This is similar to identifying ecological changes (e.g. growth) in each individual plant species which have not experienced fire [45,46].

The Soil Moisture Index (SMI) has been shown to be an indicator of topsoil moisture content in agricultural land [27,47]. However, SMI suitability for evaluating the soil moisture content in other ecosystems (i.e. swamps) has not been studied. The strong agreement between measured soil moisture contents and SMI values of the selected THPSS (Figure 9) revealed that Soil Moisture Index can reflect soil moisture contents of THPSS topsoil. This study highlighted that remote sensing technique can be used as a tool for assessing soil moisture fluctuations of THPSS topsoil for both swamps which have been mined under and non-mined under. Although SMI values cannot represent the moisture contents of soils deeper into the profile, there is a functional relationship characterized by the water retention curve between soil moisture in some (shallow) depth and the water content at the soil surface. The SMI values, therefore, can present the soil moisture status and broad recovery patterns of THPSS swamps' hydrology.

This study revealed that remote sensing can be used as a tool for assessing post fire recovery of THPSS swamps, both mined under and non-mined under swamps. In this study, we aimed to assess the broad pattern of post fire recovery for the swamps' vegetation communities, and so the aforementioned limitations of remote sensing technique did not affect this understanding. However, frequent vegetation surveys as a further study is recommended to determine the ecological changes in each individual plant species. This study suggests the potential application of remote sensing technique to understand the fire impact on vegetation and soil moisture changes in both national and global THPSS swamps and peatlands, particularly where the physical access to the site is not possible.

5. Conclusions

The post fire recovery of mined under THPSS is unknown as the mining-induced drainage may create a drier soil moisture condition and leave the swamps at a greater risk of vegetation loss due to fire. New insights from this research included the evaluation of post fire recovery (in terms of vegetation and hydrology) for mined under THPSS and non-mined under THPSS and assessment of remote sensing technique as a tool assisting with understanding post fire recovery. This study highlighted the importance of remote sensing technique, and it concluded that remote sensing indices and imagery can be used as a tool to evaluate the post fire recovery of THPSS, both mined under and non-mined under swamps. The NDVI and SMI values derived from satellite imagery of THPSS can present broad recovery patterns of swamp vegetation and hydrology. This study indicated that the vegetation recovery of mined under swamps are slower compared to the vegetation recovery of non-mined under swamps, and the post fire vegetation recovery also depends on the post fire hydrology of swamps.

Author Contributions: Conceptualization, and methodology, MS; software, MA and NU, validation, PM; formal analysis and investigation, MA and MS, resources, MS.; data curation, MA.; writing—original draft preparation, MS and MA; writing—review and editing PM, MS, TB and NM; visualization, MS, MA, PM, NM and TB.; supervision, MS, TB and NM.; project administration, MA and MS.; funding acquisition, MS. All authors have read and agreed to the published version of the manuscript.

 doi:10.20944/preprints202410.2016.v1

Funding: This research was funded by Australian Coal Association Research Program, Australia, grant number C33028.

Conflicts of Interest: The authors declare no conflicts of interest.

Appendix A

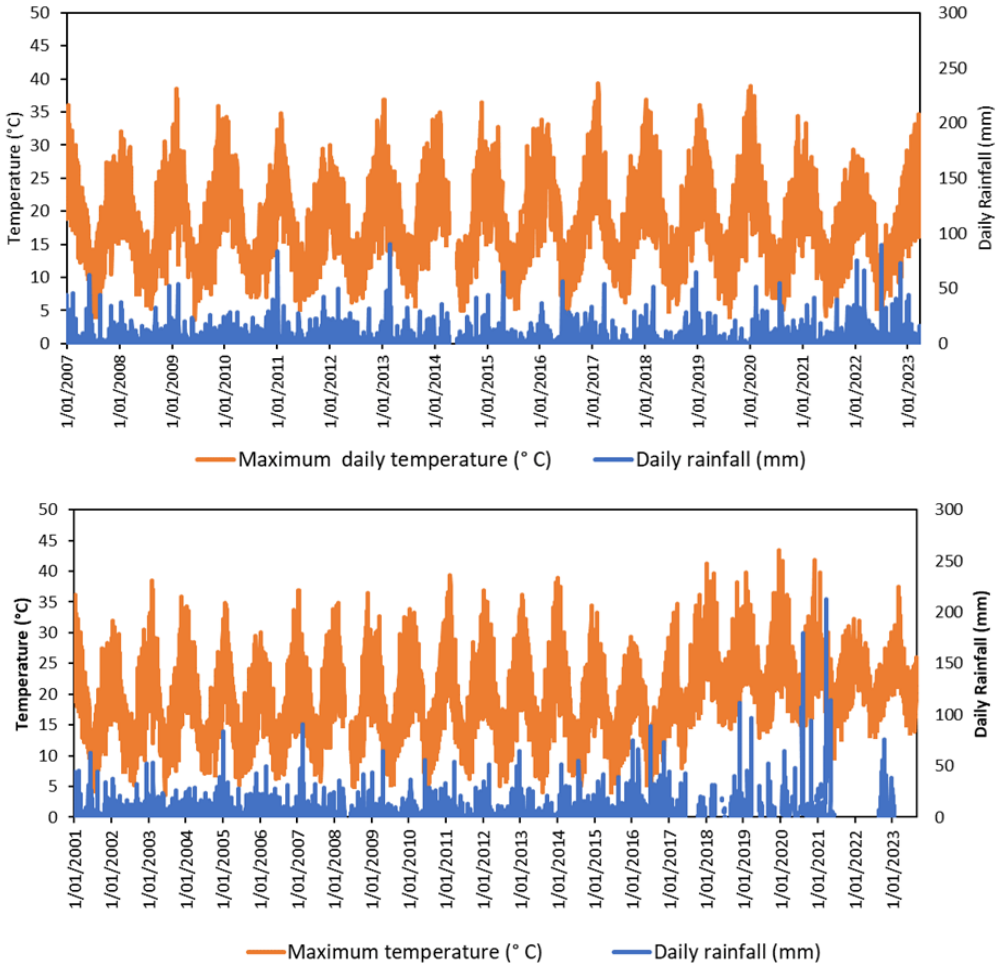

Figure A1. Air temperature and daily rainfall data for (a) Newnes Plateau before and after the fire in 2019 and (b) Upper Nepean before and after the fire in 2020 [48].

Table A1. Details for imagery used in calculation of remote sensing indices.

Source	Purpose	Spatial resolution	Temporal
Planet	Fire severity mapping using NDVI, dNDVI	3m	Daily
Aerial imagery	Validation of fire severity maps	0.05m	On request
Landsat5/7/8 OLI	NDVI, NBR time series comparison, SMI, LST	30m & 90m (thermal)	16 days
ASTER	Emissivity for LST	30m	On request

Table A2. Fire severity rankings used in the API ground-truthing based on Gibson, et al. [26].

Severity Ranking	Description	Interpretation cues (false colour infra-red aerial photos) severity	% foliage fire affected

 doi:10.20944/preprints202410.2016.v1

Extreme	Full canopy consumption	Mostly black and dark grey, largely no canopy cover	>50% canopy biomass consumed
High	Full canopy scorch (±partial canopy consumption)	No green or orange, but an even brown colour in tree canopies	>90% canopy scorched < 50% canopy biomass consumed
Moderate	Partial canopy scorch	A mixture of green, orange and brown colours in tree canopies	20–90% canopy scorch
Low	Burnt surface with unburnt canopy	Dark grey (burnt understorey) between the dark red tree crowns	>10% burnt understory >90% green canopy
Unburnt	Unburnt surface with green canopy	Dark red (live understorey) between the dark red tree crowns	0% canopy and understory burnt

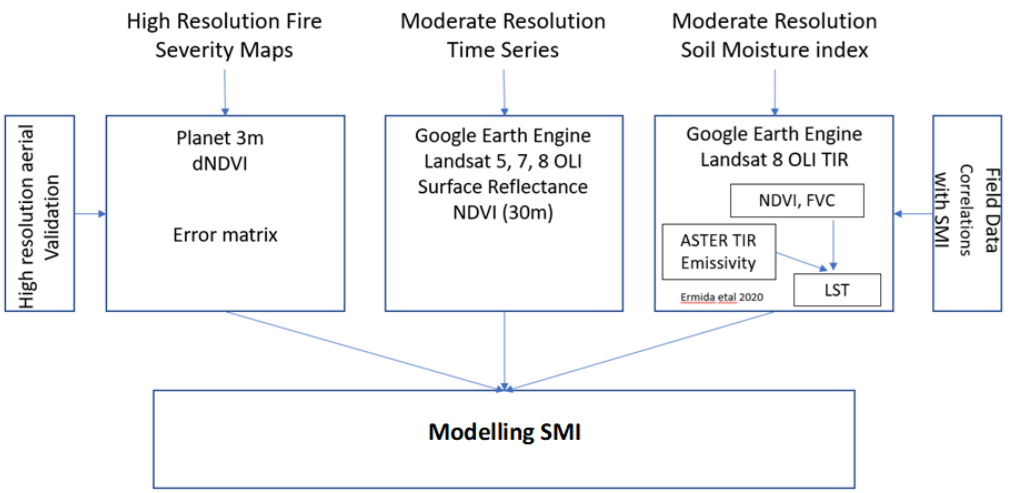

Figure A2. The Diagram indicating the process of calculating NDVI, dNDVI and SMI.

Table A3. Confusion Matrix of Swamp A and B classified fire severity map.

Class	Unburnt	Low	Moderate	High	Extreme	Total	User Accuracy	Kappa
Unburnt	67	39	1	0	0	107	0.63	
Low	0	50	15	0	0	65	0.77	
Moderate	0	1	74	8	0	83	0.89	
High	0	0	3	56	14	73	0.77	
Extreme	0	0	0	0	26	26	1	
Total	67	90	93	64	40	354		
Producer Accuracy	1	0.56	0.80	0.88	0.65		0.77	
Kappa								0.71

Table A4. Soil hydrological properties of Newnes Plateau study site.

 doi:10.20944/preprints202410.2016.v1

Location	Fire Severity	Soil properties			
		Hydraulic conductivity (cm/s)	Total porosity (cm^3/cm^3)	Macro-pore Volume (cm^3/cm^3)	Plant available water (cm^3/cm^3)
Newnes Plateau	High	0.002a	0.56a	0.18a^{ns}	0.17a
	Moderate	0.002a	0.56a	0.17a	0.18a
	Low	0.003a^{ns}	0.57a^{ns}	0.18a	0.18a^{ns}

ns: non-significant at p <0.05 (One way ANOVA test followed by a post-hoc test).

References

1. Young, A. Upland swamps in the Sydney region; Ann Young: Thirroul, Australia, 2017.
2. Shaygan, M.; Baumgartl, T.; McIntyre, N. Characterising soil physical properties of selected Temperate Highland Peat Swamps on Sandstone in the Sydney Basin Bioregion. Journal of Hydrology: Regional Studies 2022, 40, 101006.
3. Cowley, K.L.; Fryirs, K.A.; Hose, G.C. The hydrological function of upland swamps in eastern Australia: The role of geomorphic condition in regulating water storage and discharge. Geomorphology 2018, 310, 29-44.
4. Fryirs, K.A.; Cowley, K.; Hose, G.C. Intrinsic and extrinsic controls on the geomorphic condition of upland swamps in Eastern NSW. Catena 2016, 137, 100-112.
5. Mason, T.; Krogh, M.; Popovic, G.; Glamore, W.; Keith, D. Persistent effects of underground longwall coal mining on freshwater wetland hydrology. Science of The Total Environment 2021, 772, 144772.
6. Mason, T.; Keith, D.; Letten, A. Detecting state changes for ecosystem conservation with long-term monitoring of species composition. Ecological Applications 2017, 27, 458-468.
7. Keith, D.; Myerscough, P. Floristics and soil relations of upland swamp vegetation near Sydney. Australian Journal of Ecology 1993, 18, 325-344.
8. Boisramé, G.; Thompson, S.; Collins, B.; Stephens, S. Managed wildfire effects on forest resilience and water in the Sierra Nevada. Ecosystems 2017, 20, 717-732.
9. Johnstone, J.F.; Hollingsworth, T.N.; CHAPIN III, F.S.; Mack, M.C. Changes in fire regime break the legacy lock on successional trajectories in Alaskan boreal forest. Global change biology 2010, 16, 1281-1295.
10. Parks, S.A.; Holsinger, L.M.; Voss, M.A.; Loehman, R.A.; Robinson, N.P. Mean composite fire severity metrics computed with Google Earth Engine offer improved accuracy and expanded mapping potential. Remote Sensing 2018, 10, 879.
11. Wing, M.G.; Burnett, J.D.; Sessions, J. Remote sensing and unmanned aerial system technology for monitoring and quantifying forest fire impacts. Int. J. Remote Sens. Appl 2014, 4, 18-35.
12. Lentile, L.B.; Smith, A.M.; Hudak, A.T.; Morgan, P.; Bobbitt, M.J.; Lewis, S.A.; Robichaud, P.R. Remote sensing for prediction of 1-year post-fire ecosystem condition. International Journal of Wildland Fire 2009, 18, 594-608.
13. Hall, R.J.; Freeburn, J.; De Groot, W.; Pritchard, J.; Lynham, T.; Landry, R. Remote sensing of burn severity: experience from western Canada boreal fires. International Journal of Wildland Fire 2008, 17, 476-489.
14. Planet. Mapping and GIS Imagery with Planet. Available online: https://www.planet.com/ (accessed on 15 Febrauary).
15. Ibrahim, S.a.; Kose, M.; Adamu, B.; Jega, I.M. Remote sensing for assessing the impact of forest fire severity on ecological and socio-economic activities in Kozan District, Turkey. Journal of Environmental Studies and Sciences 2024, 1-13.
16. Schag, G.M.; Stow, D.A.; Riggan, P.J.; Tissell, R.G.; Coen, J.L. Examining landscape-scale fuel and terrain controls of wildfire spread rates using repetitive airborne thermal infrared (ATIR) imagery. Fire 2021, 4, 6.
17. San-Miguel, I.; Andison, D.W.; Coops, N.C. Characterizing historical fire patterns as a guide for harvesting planning using landscape metrics derived from long term satellite imagery. Forest Ecology and Management 2017, 399, 155-165.
18. Stow, D.; Riggan, P.; Schag, G.; Brewer, W.; Tissell, R.; Coen, J.; Storey, E. Assessing uncertainty and demonstrating potential for estimating fire rate of spread at landscape scales based on time sequential airborne thermal infrared imaging. International Journal of Remote Sensing 2019, 40, 4876-4897.
19. Schag, G.M.; Stow, D.A.; Riggan, P.J.; Nara, A. Spatial-statistical analysis of landscape-level wildfire rate of spread. Remote Sensing 2022, 14, 3980.

20. Bureau of Meteorology. Climate data Available online: http://www.bom.gov.au/climate/data/index.shtml (accessed on 18/05/2023).
21. ecoTech. Tensiomark. Available online: https://www.ecotech-bonn.de/en/produkte/bodenkunde/Bodenfeuchte/wasserspannung/tensiomark/ (accessed on
22. Sentek Pty Ltd. Calibration manual for sentek soil moisture sensors. Available online: http://data.hydrolina.ch/manuals/Calibration/Calibration%20Manual%20V2.0.pdf (accessed on 16 September).
23. Ozyavuz, M.; Bilgili, B.; Salici, A. Determination of vegetation changes with NDVI method. Journal of environmental protection and ecology 2015, 16, 264-273.
24. Carlson, T.N.; Gillies, R.R.; Perry, E.M. A method to make use of thermal infrared temperature and NDVI measurements to infer surface soil water content and fractional vegetation cover. Remote sensing reviews 1994, 9, 161-173.
25. Rouse, J.W.; Haas, R.H.; Schell, J.A.; Deering, D.W. Monitoring vegetation systems in the Great Plains with ERTS. NASA Spec. Publ 1974, 351, 309.
26. Gibson, R.; Danaher, T.; Hehir, W.; Collins, L. A remote sensing approach to mapping fire severity in south-eastern Australia using sentinel 2 and random forest. Remote Sensing of Environment 2020, 240, 111702.
27. Saha, A.; Patil, M.; Goyal, V.C.; Rathore, D.S. Assessment and impact of soil moisture index in agricultural drought estimation using remote sensing and GIS techniques. In Proceedings of the Proceedings, 2018; p. 2.
28. Khan, A.; Chatterjee, S.; Weng, Y. Characterizing thermal fields and evaluating UHI effects. In Urban Heat Island Modeling for Tropical Climates; 2021; pp. 37-67.
29. Ermida, S.L.; Soares, P.; Mantas, V.; Göttsche, F.-M.; Trigo, I.F. Google earth engine open-source code for land surface temperature estimation from the landsat series. Remote Sensing 2020, 12, 1471.
30. Hulley, G.C.; Hook, S.J.; Abbott, E.; Malakar, N.; Islam, T.; Abrams, M. The ASTER Global Emissivity Dataset (ASTER GED): Mapping Earth's emissivity at 100-meter spatial scale. Geophysical Research Letters 2015, 42, 7966-7976.
31. Carlson, T.N.; Ripley, D.A. On the relation between NDVI, fractional vegetation cover, and leaf area index. Remote sensing of Environment 1997, 62, 241-252.
32. Sun, J.; Wang, X.; Chen, A.; Ma, Y.; Cui, M.; Piao, S. NDVI indicated characteristics of vegetation cover change in China's metropolises over the last three decades. Environmental monitoring and assessment 2011, 179, 1-14.
33. Aburas, M.M.; Abdullah, S.H.; Ramli, M.F.; Ash'aari, Z.H. Measuring land cover change in Seremban, Malaysia using NDVI index. Procedia Environmental Sciences 2015, 30, 238-243.
34. Keith, D.A.; Myerscough, P.J. Floristics and soil relations of upland swamp vegetation near Sydney. Australian Journal of Ecology 1993, 18, 325-344, doi:10.1111/j.1442-9993. 1993.tb00460.x.
35. Lukenbach, M.C.; Devito, K.J.; Kettridge, N.; Petrone, R.M.; Waddington, J.M. Hydrogeological controls on post-fire moss recovery in peatlands. Journal of Hydrology 2015, 530, 405-418, doi:https://doi.org/10.1016/j.jhydrol.2015.09.075.
36. Lukenbach, M.C.; Hokanson, K.J.; Moore, P.A.; Devito, K.J.; Kettridge, N.; Thompson, D.K.; Wotton, B.M.; Petrone, R.M.; Waddington, J.M. Hydrological controls on deep burning in a northern forested peatland. Hydrological Processes 2015, 29, 4114-4124, doi:10.1002/hyp.10440.
37. Lukenbach, M.C.; Hokanson, K.J.; Devito, K.J.; Kettridge, N.; Petrone, R.M.; Mendoza, C.A.; Granath, G.; Waddington, J.M. Post-fire ecohydrological conditions at peatland margins in different hydrogeological settings of the Boreal Plain. Journal of Hydrology 2017, 548, 741-753, doi:https://doi.org/10.1016/j.jhydrol.2017.03.034.
38. Lukenbach, M.C.; Devito, K.J.; Kettridge, N.; Petrone, R.M.; Waddington, J.M. Burn severity alters peatland moss water availability: implications for post-fire recovery. Ecohydrology 2016, 9, 341-353, doi:10.1002/eco.1639.
39. Lacouture, D.L.; Broadbent, E.N.; Crandall, R.M. Detecting vegetation recovery after fire in a fire-frequented habitat using normalized difference vegetation index (NDVI). Forests 2020, 11, 749.
40. Alcañiz, M.; Outeiro, L.; Francos, M.; Úbeda, X. Effects of prescribed fires on soil properties: A review. Science of the Total Environment 2018, 613, 944-957.
41. Moody, J.A.; Ebel, B.A.; Nyman, P.; Martin, D.A.; Stoof, C.; McKinley, R. Relations between soil hydraulic properties and burn severity. International Journal of Wildland Fire 2016, 25, 279-293, doi:https://doi.org/10.1071/WF14062.
42. McKenna, P.; Phinn, S.; Erskine, P.D. Fire severity and vegetation recovery on mine site rehabilitation using WorldView-3 imagery. Fire 2018, 1, 22.
43. Wilson, N.R.; Norman, L.M. Analysis of vegetation recovery surrounding a restored wetland using the normalized difference infrared index (NDII) and normalized difference vegetation index (NDVI). International Journal of Remote Sensing 2018, 39, 3243-3274.

 doi:10.20944/preprints202410.2016.v1

44. Veraverbeke, S.; Gitas, I.; Katagis, T.; Polychronaki, A.; Somers, B.; Goossens, R. Assessing post-fire vegetation recovery using red–near infrared vegetation indices: Accounting for background and vegetation variability. ISPRS Journal of Photogrammetry and Remote Sensing 2012, 68, 28-39.
45. Hernandez-Santin, L.; Rudge, M.L.; Bartolo, R.E.; Erskine, P.D. Identifying species and monitoring understorey from UAS-derived data: A literature review and future directions. Drones 2019, 3, 9.
46. Fletcher, A.T.; Erskine, P.D. Mapping of a rare plant species (Boronia deanei) using hyper-resolution remote sensing and concurrent ground observation. Ecological Management & Restoration 2012, 13, 195-198, doi:https://doi.org/10.1111/j.1442-8903.2012.00649.x.
47. Carrão, H.; Russo, S.; Sepulcre-Canto, G.; Barbosa, P. An empirical standardized soil moisture index for agricultural drought assessment from remotely sensed data. International journal of applied earth observation and geoinformation 2016, 48, 74-84.
48. BOM, B.o.M. Annual and monthly potential frost days. 2023.